# Terahertz pulse generation and detection with LT-GaAs photoconductive antenna

J. Zhang, Y. Hong, S.L. Braunstein and K.A. Shore

**Abstract:** The characteristics of optically induced teraherz (THz) radiation from a biased low-temperature-grown GaAs (LT-GaAs) photoconductive antenna were investigated using a femtosecond Ti:sapphire laser. The THz pulse radiation from two different LT-GaAs photoconductive antennas were compared and two kinds of THz waveform were observed. Saturation behaviour of the emission of THz radiation is observed by using a CW laser diode to optically pre-bias the emitter antenna.

## 1 Introduction

The generation and detection of terahertz (THz) radiation using ultrashort pulses has been intensively studied during the last decade. THz pulses have found many applications, such as THz imaging, THz time-domain spectroscopy for studies of carrier dynamics and intermolecular dynamics in liquids, and dielectric responses of molecules, polymers, and semiconductors. The generation of THz radiation has been achieved by various techniques, such as ultrafast switching of photoconductive antennas [1, 2], rapid screening of the surface field via photoexcitation of dense electron hole plasma in semiconductors [3], rectification of optical pulses in crystals [4], carrier tunnelling in coupled double-quantum well structures [5] and coherent excitation of polar optical photons [6]. Of these various methods, photoconductive antennas have proved to be a promising source of THz radiation with respect to both the intensity and spectral bandwidth. Low-temperature-grown GaAs (LT-GaAs) has been the most widely used material for the photoconductive emitter and detector because of its unique properties, such as the ultrashort carrier lifetime, large resistivity, and relatively good carrier mobility. When a biased LT-GaAs antenna is pumped by ultrafast laser pulses, the rapid change of the transport photocurrent gives rise to electromagnetic radiation. The THz electromagnetic radiation arises from two processes: the acceleration of the photogenerated carrier under a biased electric field and the rapid change of the carrier density via femtosecond laser pumping. The emitted THz waveforms and frequency spectrum of the biased LT-GaAs photoconductive antenna have been studied by several groups [7–10]. Emitted waveforms exhibiting W-shape and bipolar characteristics have been observed experimentally. The reasons for the different characteristics exhibited by the emitted wave-forms has been the subject of some discussion [11, 12]. In this paper, we report a study on the waveforms characteristics of THz radiation generated and detected using LT-GaAs photoconductive antennas. Two distinct THz waveforms were observed by employing various emitters provided by two groups. In addition we have observed the amplitude and wave-form of THz radiation obtained by applying an optical 'pre-bias' provided by illumination using a CW laser diode.

## 2 Experiment

The experimental setup to generate and detect beams of short pulses of THz radiation is shown in Fig. 1. It consists of a femtosecond laser, an optical delay line, an optical chopper, a THz emitter, a set of off-axis paraboloidal mirrors for collimating and focusing the THz beam, a low-noise current preamplifier, and a lock-in amplifier. A CW diode-pumped, regenerative mode-locked Ti:sapphire laser (Mai Tai, Spectra-Physics), which gives a 100-fs pulse duration with $>700\,\mathrm{mW}$ of average power and an 80 MHz repetition rate, was used to generate THz radiation. A single-mode laser diode operating at a wavelength of $\sim 830\,\mathrm{nm}$ is used to produce the constant carriers in the emitter antenna. We employ two H-shaped photomixer antennas as the THz emitter and detector. The LT-GaAs layer grown on a semi-insulating GaAs wafer was used as the photoconductor. The metal patterns are deposited on the LT-GaAs layer. Figure 1b shows schematically the photoconductive antenna with a dipole shape. The photomixer antennas were fabricated with dipole length $L$ and small photoconductive gap $(5\,\mu\mathrm{m})$ located at the centre of an approximately 10-mm-long coplanar transmission line. The photomixer antennas with dipole length $L = 400\,\mu\mathrm{m}$, $200\,\mu\mathrm{m}$ for the emitter and $300\,\mu\mathrm{m}$ for the detector were provided by T. Kleine-Ostmann at Technische University Braunschweig, Germany, and the $L = 20\,\mu\mathrm{m}$ for the emitter by K. Sakai at Communications Research Laboratory, Japan. A hemispherical silicon lens which was made of high-resistivity $(>10\,\mathrm{k\Omega\,cm})$ silicon with a diameter of 9 mm was attached to the back of the 0.4-mm-thick GaAs substrate of the antenna device in order to reduce the reflection loss at the air–substrate interface and to increase the radiation collection efficiency.

45 mW of average laser power is separated into two beams with a 50/50 beam-splitter cube. One optical beam is

The authors are with the School of Informatics, Bangor University, Bangor LL57 1UT, UK

J. Zhang is also with the State Key Laboratory of Quantum Optics and Quantum Optics Devices, Institute of Opto-Electronics, Shanxi University, Taiyuan 030006, People's Republic of China
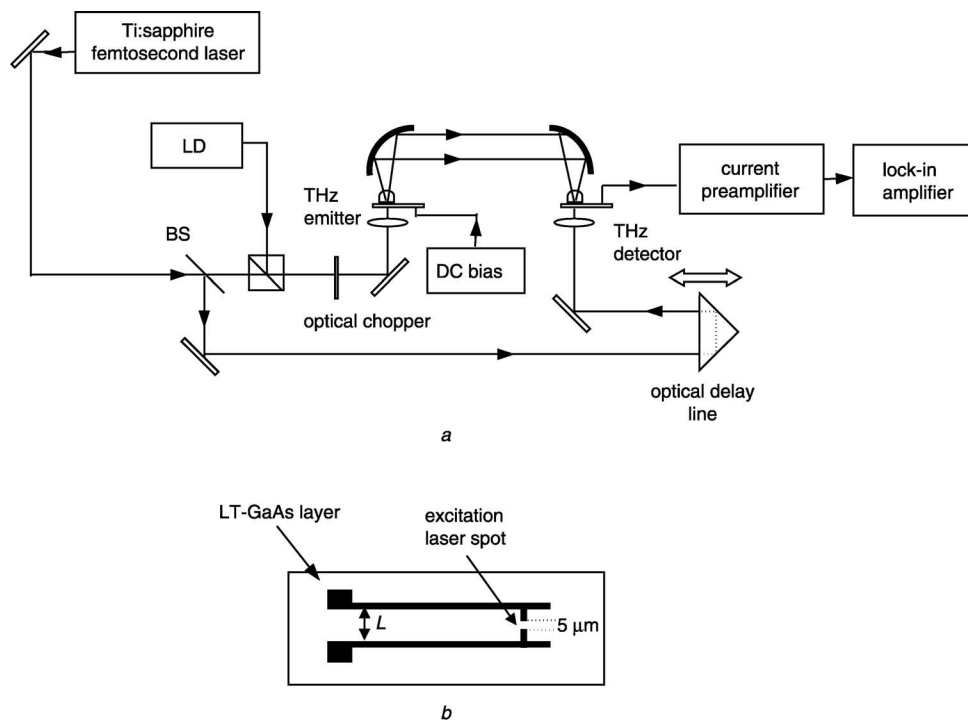
**Fig. 1** *Experimental setup*

*a* Schematic of experimental setup for generation and detection of THz pulses
*b* Structure of dipole photomixer antennas fabricated on the LT-GaAs film

first combined with the light from the laser diode by a polarising beam splitter (PBS). The output beam from the PBS passes an optical chopper, and is then focused into the emitter antenna with a 6-mm focal length to excite THz pulses. A voltage of $\sim 45\,V$ is applied across the two strip lines. The generated THz radiation was emitted into free space through a silicon hemispherical substrate lens and was then collected and focused in the direction of the pump beam by a pair of 63-mm aperture off-axis parabolic mirrors of 60-mm focal length (Melles Griot). After being guided through the optical delay line consisting of a right-angle prism as the retroreflector on the high-precision translation stage, the other optical beam is focused with a 8-mm focal length to gate the detection antenna. The detection antenna with dipole length $L = 300\,\mu m$ remains unchanged in our scheme and is not DC biased. The photocurrent from the detection antenna was preamplified with a low-noise current amplifier and then detected with a lock-in amplifier reference to an optical chopper. The modulation frequency of the optical chopper was 300 Hz and the time constant of the lock-in amplifier was 30 ms.

## 3 Results

When a femtosecond laser pulse illuminates the semiconductors with a photon energy greater than the band gap, photons are absorbed, thus creating electron–hole pairs. The external biased field drives the photogenerated carriers to form a transient photocurrent across the field region. Namely, a radiated THz electric field is obtained by the time derivative of the net current. First, only the femtosecond laser illuminates the emitter antenna without the light of the laser diode. We use the dipole antenna $L = 400\,\mu m$ and $L = 200\,\mu m$ to generate sub-THz pulse radiation in Fig. 2. Figure 2a shows the THz signal waveform as a function of the delay between the optical pulse on the detection antenna and THz pulse, measured through the lock-in amplifier.
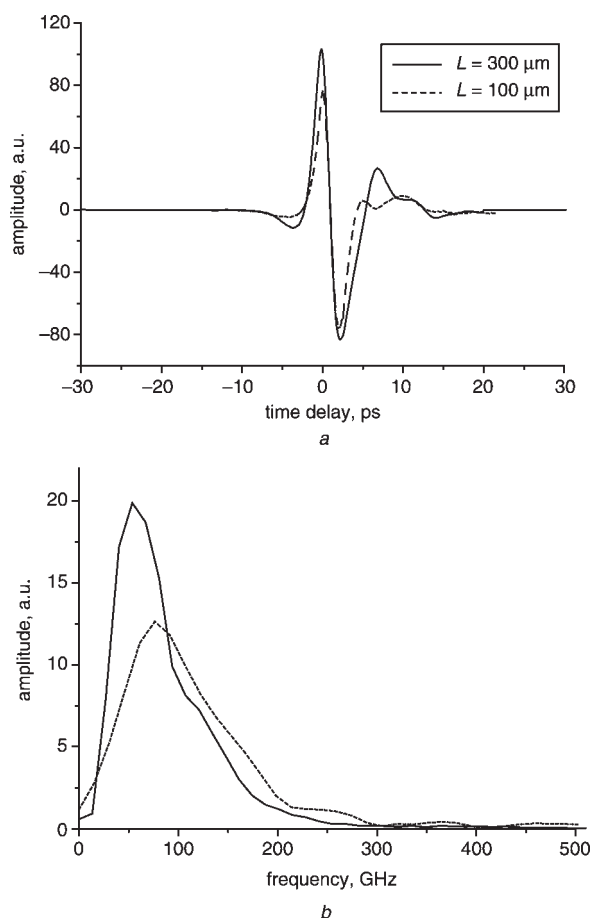


**Fig. 2** *THz pulse generation using dipole antenna with L = 300 μm and 100 μm*

*a* THz pulses from the dipole antenna measured by scanning the time delay between optical gating pulses and incident THz pulses, while monitoring output of lock-in amplifier
*b* The corresponding frequency spectrum of the measured THz pulse shape

As can be seen, the slightly asymmetrical bipolar characteristics of the THz radiation waveforms is independent of emitter dipole length and only the peak strength of the emitted THz field changed. Figure 2b shows the Fourier transformed spectrum of the detected signal THz waveform shown in Fig. 2a. The spectral peak is located at around 100 GHz and the radiation frequency spectrum extends to 0.5 THz. Comparing the spectra of the 400 µm dipole antenna with 200 µm, the spectrum of the longer dipole antenna has a higher peak, broader frequency band and lies in lower-frequency regions. The long dipole antenna processes a sharp resonant structure due to the high Q-value of the antenna. Figure 3 shows the waveform and frequency spectrum with the emitter dipole length $L = 20$ µm. The radiation frequency spectrum extends to 1 THz; however, the spectral peak value is only one-sixth of that from the emitter of dipole length $L = 400$ µm. The detected signal THz waveform shown in Fig. 3a exhibit slightly asymmetrical W-shape characteristics, which is quite distinct from that shown in Fig. 2a. The characteristics of the THz waveform do not alter when we change the size of the laser spot and pumping power. This suggests that the characteristics of the LT-GaAs ultimately determine the shape of the THz waveform. As the CW laser diode illuminates the emitter antenna and generates the constant carriers, the two kinds of THz pulse waveforms remain unchanged, but the amplitude of the emitted THz pulse increases. In Fig. 4, we show the influence on the peak THz

amplitude as the pump power of the laser diode increases. The peak THz field shows clear saturation behaviour as a function of the CW pump influence. The peak THz amplitude will increase linearly when the density of the optically injected carriers is low. However, when the pump power of the laser diode is larger than $\sim 12$ mW (the saturated power depends on the power of the femtosecond pump pulse and the biased voltage), the THz pulses amplitude shows saturation.
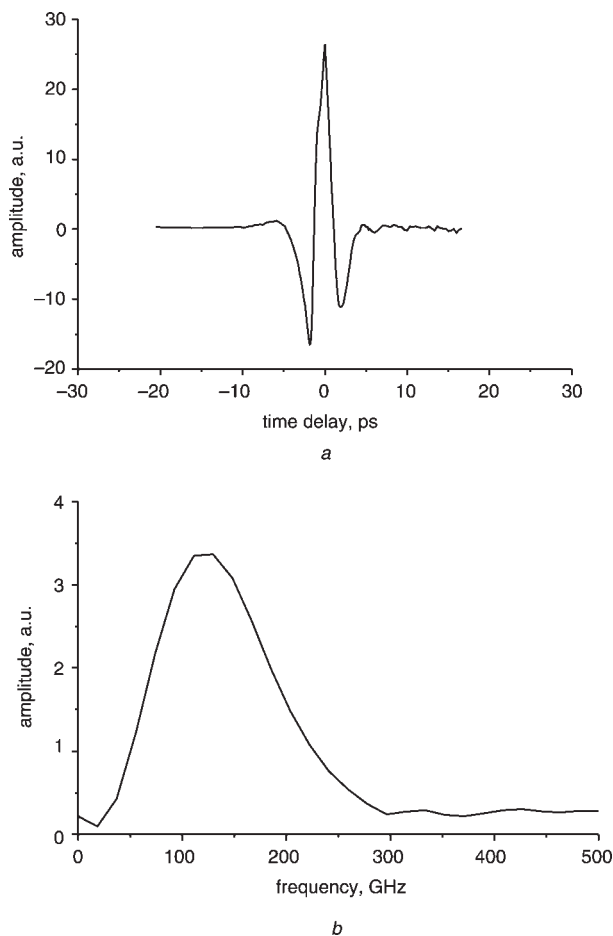


**Fig. 4** *Peak THz amplitude as a function of pump power of the CW laser diode*





**Fig. 3** *THz pulse generation using dipole antenna with $L = 20$ µm*

*a* THz pulses from the dipole antenna $L = 20$ µm measured by scanning the time delay between optical gating pulses and incident THz pulses, while monitoring output of lock-in amplifier
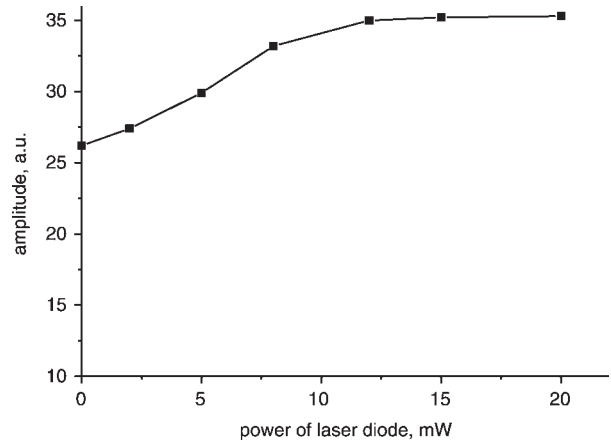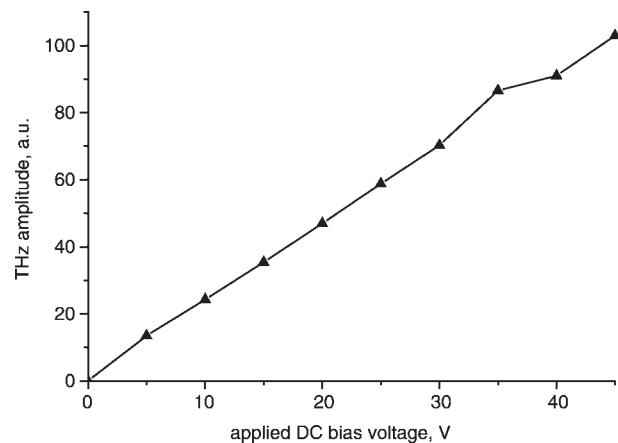*b* The corresponding frequency spectrum of the measured THz pulse shape



**Fig. 5** *Maximum THz signal at output of lock-in amplifier against bias voltage on the photoconductive antennas*
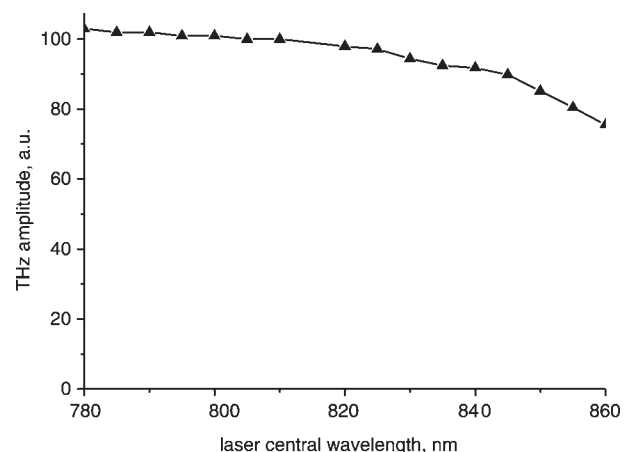


**Fig. 6** *Maximum THz signal at the output of lock-in amplifier against central wavelength of femtosecond Ti:sapphire laser*
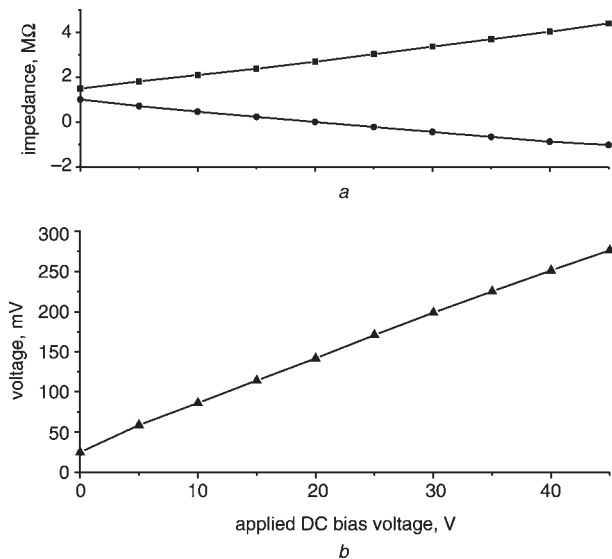
**Fig. 7** *Impedance and output voltage of the detection antenna against the bias voltage of the emitter antenna*

*a* Impedance
*b* Output voltage

Figure 5 plots the measured peak value of terahertz pulses versus the bias voltage on the photoconductive antenna (dipole length $L = 400\,\mu m$). It is evident that the strength of generated pulses is proportional to the biased voltage of the emitter antenna. We observed the strength of the THz radiation by changing the central wavelength of the femto-second laser. Figure 6 shows the dependence of the strength of THz radiation via the central wavelength of the pump laser. The strength of the THz radiation decreases when the central wavelength of the pump laser increases. Electron–hole pairs are generated when an optical gate pulse illuminates the detector in the gap of the dipole antenna. These carriers are driven by the THz electric field, producing a current, the magnitude of which is proportional to the THz field and the carrier concentration and the direction of which is determined by the polarity of the THz field. The detection antenna may be regarded as the RC circuit including the current source. We measure the impedance and output voltage of the detection antenna directly using the multimeter. The two curves in Fig. 7*a* show the measured impedance of the detector antenna under different detection polarities of the multimeter. The polarity of the detection antenna influences the measured impedance with the multimeter. Figure 7*b* shows a plot of the output voltage of the detection antenna as a function of the bias voltage of the emitter antenna. It is evident that the output voltage of the detection antenna is proportional to the magnitude of the THz field.

In conclusion, we have studied the generation of electromagnetic wave pulses in the sub-THz frequency region from voltage-biased photoconductive antennas excited with a femtosecond Ti:sapphire laser. The photo-conductive emitter fabricated by two groups generated two distinctive different THz waveforms. It was observed that the THz waveform remained unchanged on varying the optical excitation influence, the strength of the biased field and the emitter gap spacing. This shows the shape of the THz waveform is determined by the characteristics of LT-GaAs.

## 5 References

1 Auston, D.H., Cheung, K.P., and Smith, P.R.: 'Picosecond photo-conducting hertzian dipoles', *Appl. Phys. Lett.*, 1984, **45**, (3), pp. 284–286
2 Grischkowsky, D., Keiding, S., Vanexter, M., and Fattinger, C.: 'Far-infrared time-domain spectroscopy with terahertz beams of dielectrics and semiconductors', *J. Opt. Soc. Am. B*, 1990, **7**, (10), pp. 2006–2015
3 Zhang, X.C., and Auston, D.H.: 'Optoelectronic measurement of semiconductor surfaces and interfaces with femtosecond optics', *J. Appl. Phys.*, 1992, **71**, (1), pp. 326–338
4 Hu, B.B., Zhang, X.C., Auston, D.H., and Smith, P.R.: 'Free-space radiation from electrooptic crystals', *Appl. Phys. Lett.*, 1990, **56**, (6), pp. 506–508
5 Roskos, H.G., Nuss, M.C., Shah, J., Leo, K., Miller, D.A.B., Fox, A.M., Schmit-Trink, S., and Kohler, K.: 'Coherent submillimeter-wave emission from charge oscillations in a double-well potential', *Phys. Rev. Lett.*, 1994, **68**, (14), pp. 2216–2219
6 Tani, M., Fukasawa, R., Abe, H., Matsuura, S., Sakai, K., and Nakashima, S.: 'Terahertz radiation from coherent phonons excited in semiconductors', *J. Appl. Phys.*, 1998, **83**, (5), pp. 2473–2477
7 Pedersen, J.E., Lyssenko, V.G., Hvam, J.M., Jepsen, P.U., Keiding, S.R., Sorensen, C.B., and Lindelof, P.E.: 'Ultrafast local field-dynamics in photoconductive THz antennas', *Appl. Phys. Lett.*, 1993, **62**, (11), pp. 1265–1267
8 Cai, Y., Brener, I., Lopata, J., Wynn, J., Pfeiffer, L., and Federici, J.: 'Design and performance of singular electric field terahertz photo-conducting antennas', *Appl. Phys. Lett.*, 1997, **71**, (15), pp. 2076–2078
9 Brener, I., Dykaar, D., Frommer, A., Pfeiffer, L.N., Lopata, J., Wynn, J., West, K., and Nuss, M.C.: 'Terahertz emission from electric field singularities in biased semi-conductors', *Opt. Lett.*, 1996, **21**, (23), pp. 1924–1926
10 Lin, P.I., Chen, S.F., Wu, K.H., Juang, J.Y., Uhn, T.M., and Gou, Y.S.: 'Characteristics of photogenerated bipolar terahertz radiation in biased photoconductive switches', *Jpn. J. Appl. Phys.*, 2002, **41**, (10B), pp. L1158–L1160
11 Rodriguez, G., and Taylor, A.J.: 'Screening of the bias field in terahertz generation from photoconductors', *Opt. Lett.*, 1996, **21**, (14), pp. 1046–1048
12 Piao, Z.S., Tani, M., and Sakai, K.: 'Carrier dynamics and terahertz radiation in photoconductive antennas', *Jpn. J. Appl. Phys.*, 2000, **39**, (1), pp. 96–100